THE JOURNAL OF PHYSICAL CHEMISTRY B

Article

pubs.acs.org/JPCB

Kinetic Model for the Activation of Mammalian Olfactory Receptor

Seogjoo Jang*[,†,‡] and Changbong Hyeon[§]

[†]Department of Chemistry and Biochemistry, Queens College, City University of New York, 65-30 Kissena Boulevard, Queens, New York 11367, United States

[‡]PhD programs in Chemistry and Physics, and Initiative for Theoretical Sciences, Graduate Center, City University of New York, 365 Fifth Avenue, New York, New York 10016, United States

[§]School of Computational Sciences, Korea Institute for Advanced Study, Hoegiro 85, Dongdaemun-gu, Seoul 02455, Korea

ABSTRACT: The sense of smell is triggered by binding of odorants to a set of olfactory receptors (ORs), the activation of which generates specific patterns of neuronal signals in olfactory bulbs. Despite a long history of research and speculations, very little is known about the actual mechanism of OR activation. In particular, there is virtually no theoretical framework capable of describing the kinetics of olfactory activation at a quantitative level. Based on the fact that mammalian ORs belong to a class of G-protein coupled receptors (GPCRs) and utilizing the information available from recent studies on other types of GPCRs with known structural data, we construct a minimal kinetic model for mammalian olfactory activation, obtaining a new expression for the signal strength as a function of odorant and G-protein concentrations and defining this as odor activity (OA). The parametric dependence of OA on equilibrium dissociation and rate constants provides a new comprehensive means to describe how odorant-OR binding kinetics affects the odor signal, and offers new quantitative criteria for classifying agonistic, partially agonistic, and antagonistic (or inverse agonistic) behavior. The dependence of OA on the concentration of G-proteins also suggests a new experimental method to determine key equilibrium constants for odorant-OR and G-protein-OR association/dissociation processes.

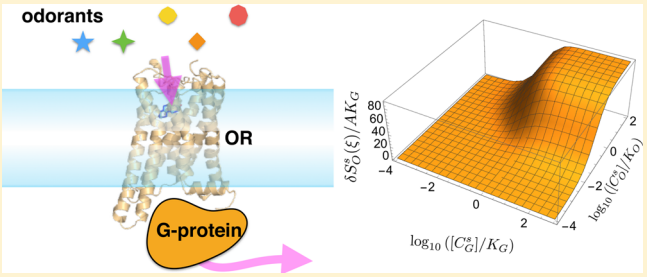

INTRODUCTION

Olfaction, nature's effective tool for chemical detection, is the most versatile sensory function animals utilize for their survival.[1−3] However, how olfaction works at a molecular level is not well understood despite its familiarity. This can be attributed to three major factors. First, other than computational studies based on homology models[4,5] and mutagenesis experiments,[6−9] little structural information is available to date for any olfactory receptor (OR), making it difficult to investigate atomistic details of OR-odorant interactions. Second, the activation of OR entails a series of biochemical amplification steps and neuronal signal processes that are too complex to fully grasp at present.[2,3,10−12] Third, odor perception data are difficult to quantify in a systematic and objective manner, and no consensus exists at present on the dimensionality and characteristics of the odor space.[13−15] As a result, theories of olfaction have remained largely speculative, relying heavily on unconfirmed assumptions and simple analogies. In particular, which molecular features of odorants play major roles in the activation of ORs has remained a highly contentious issue.

There have been various theories proposing widely different mechanisms[1] of odorant detection. The most well-known theory of olfactory activation is stereochemical theory (SCT),[1,16,17] which assumes that each OR is activated by a lock-and-key type structural fit of odorant. Profile-functional group theory (PFT)[1,18] assumes that the form, shape, size, and functional groups of odorants can all play important roles. On the contrary, vibrational theory (VT)[19−22] proposes that ORs are activated by specific vibrational frequencies of odorants.

Although SCT seems to capture the gist of odorant-OR interactions and has been successful to some degree, it falls short of providing a comprehensive and reliable description of olfactory sensing.[23] This is understandable considering that the assumption underlying SCT, structural fitting of odorants serving as a sole mechanism of activation, is too simplistic to represent the complexity of the chemical interaction between odorants and the active site of OR. In addition, there is a growing consensus that dynamical effects of protein-molecule interactions can be much more important than has been perceived previously.[24−26] In this regard, PFT[1,18] has the potential to better represent realistic aspects of molecular level odorant recognition. However, the current version of PFT has not yet evolved far enough from being a simple set of empirical rules, and is not based on a concrete physical model. Although various ideas[1,27] modifying SCT, for example, induced structural fit, are available, they have not yet developed into quantitative theories of olfactory activation either.

In recent years, new efforts[28−32] have been made to promote VT as an alternative theory to SCT. Despite its long history,[19]

Received: January 16, 2017
Revised: January 21, 2017
Published: January 24, 2017

DOI: 10.1021/acs.jpcb.7b00486
J. Phys. Chem. B 2017, 121, 1304−1311

VT had suffered from the lack of a plausible physical model for detecting the vibrational frequencies of odorants. Recent theoretical works[31−33] made progress in this regard by constructing electron transfer (ET) models for such detection. However, these theories still remain hypothetical because there is no evidence for the existence of ET process in the OR at present. In particular, it is not even clear whether plausible electron donor and acceptor sites can be found in actual ORs.

It is true that there are numerous examples of ET reactions in biological systems.[34−36] However, for these confirmed cases, the reason for the existence of ET reactions can be understood easily. They either provide key energy storage mechanisms following photoexcitation as in photosynthesis or serve as necessary steps of biological oxidation/reduction processes. In this sense, the assumption of VT that an electron (or a hole) is created and then discarded, simply to detect relatively small vibrational energies of molecules, appears quite peculiar. Even if we accept such an assumption, there are many reasons why an ET mechanism is likely to be incapable of detecting vibrational frequencies of odorants with high enough sensitivity, as pointed out recently.[27,37] Thus, without satisfactory account of these issues, broad acceptance of VT is not likely.[38]

A key argument for VT is the isotope effect[28−30,33] found or claimed in relation to odor sensing. However, at present, much of the experimental evidence for the isotope effect remains obscure[27,39] at best. Relatively firm, but very limited, evidence can be found for insects only,[29,33] for which details of ORs are much less known than for mammalian ones. Regardless of future experimental results that can clearly settle the existence of actual isotope effects, it is also important to note that VT is not the only theory that can potentially explain such experimental results. Any theory capable of including the effects of the dynamics and chemical interactions of odorants, involving protons and hydrogens in particular, could potentially account for isotope effects, although it may not always be easy to set predictable trends.[40,41]

The main objective of this article is to overcome limitations imposed by current theories of OR activation as summarized above, by constructing a more satisfactory theoretical model of olfactory activation that can accommodate major structural, chemical, and dynamic effects altogether, in a manner consistent with the modern viewpoint of protein-ligand interactions. A successful outcome of this modeling would result in an improvement of SCT or a new PFT with clear physical basis. This may also provide a consistent explanation of any isotope effect, if found.

At present, constructing a definite and detailed kinetic model of OR activation is difficult because no reliable structural information is available for any OR. However, at least for mammalian cases, for which ORs are known to belong to the family of G-protein coupled receptors (GPCRs),[2,42] important clues and insights can be gained from recent findings and computational studies of GPCRs with known structural information.[43−48] Insights offered from these studies will serve as the basis for a kinetic model constructed in this work. However, because many findings about GPCRs are still at formative stage and clear understanding of the key features setting ORs apart from GPCRs with known structural data is currently lacking, it seems inevitable to introduce some assumptions that remain to be validated, although reasonable. In this sense, the kinetic model being presented here is subject to further improvement and refinement, and should be considered as the first step for a long-term effort for establishing a genuinely satisfactory theoretical model.

THEORETICAL MODEL

Although there are multiple ORs of the same type embedded in the olfactory cilia of a given olfactory sensory neuron (OSN),[1,2] we here consider only a single OR and its probability of odorant detection and activation. This is because there is no evidence at present that spatial distribution of ORs and their specific locations have any major effects on the generation of signal through OSN. Thus, in the present work, we assume that all the ORs of the same type can be treated as being equivalent and independent of each other.

For a given OR, we define $P_0(t)$ as the probability to find it as a free form at time t. The probabilities to find the OR in three other different forms are denoted as $P_k(t)$'s with k = 1, 2, and 3, where $P_1(t)$ represents G-protein bound OR (OR_G), $P_2(t)$ the odorant bound OR (OR_O), and $P_3(t)$ the OR bound by both G-protein and odorant (OR_{OG}) (see Figures 1 and 2). The sum of all these probabilities is equal to one as follows:

$$\sum_{k=0}^{3} P_k(t) = 1 \tag{1}$$

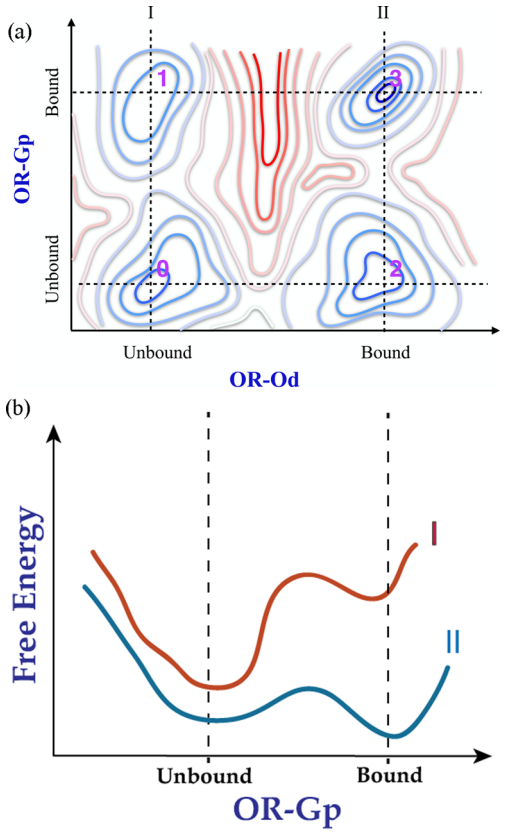

Figure 1. (a) Illustration of expected two-dimensional free energy surface with respect to the two reaction coordinates representing OR and odorant and OR and G-protein. Each basin is numbered from 0 to 3 in accordance with the labeling convention as noted in the paragraph above eq 1. (b) One dimensional sections of the free energy surfaces across two lines I and II.

DOI: 10.1021/acs.jpcb.7b00486
J. Phys. Chem. B 2017, 121, 1304−1311

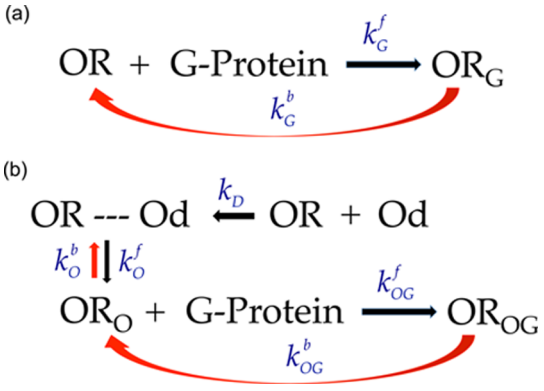

Figure 2. (a) Schematic of the rate process expected in the absence of odorants, which involves OR, G-protein, and G-protein bound OR (OR_G). k_G^f and k_G^b are rate constants for the forward and backward reactions. (b) Schematic of the additional rate process expected in the presence of odorant (Od), which also involves G-protein, odorant bound OR (OR_O), and both odorant and G-protein bound OR (OR_{OG}). The bimolecular diffusion rate constant involving OR and Od is denoted by k_D. The rate constants for forward and backward reactions involving OR, Od, and OR_O are denoted by k_O^f and k_O^b, and those involving OR_O, G-protein, and OR_{OG} are denoted by k_{OG}^f and k_{OG}^b.

Below we consider the kinetics involving these populations, first in the absence of odorants and then next in the presence of odorants.

Kinetics without Odorants. In the absence of odorants, we suppose that the activation of OR can be represented by the following rate equation (see Figures 1b and 2a):

$$\frac{dP_0(t)}{dt} = -k_G^f C_G(t) P_0(t) + k_G^b P_1(t) \tag{2}$$

where k_G^f is the bimolecular reaction rate for the formation of OR_G, k_G^b is the rate for the G-protein to dissociate back from OR_G, and $C_G(t)$ is the (number) concentration of the G-protein in the vicinity of the OR. As is illustrated in Figure 1b, we expect that k_G^f is smaller than k_G^b. This way, the majority of the population of ORs would be available for activation by odorants.

Because a downstream signal is generated by the release of G-protein from OR_G, the basal signal being produced by the OR in the absence of odorant is given by

$$S_b(t) = A k_G^b P_1(t) \tag{3}$$

where A reflects both the fraction of dissociating G-protein that leads to signal production and the amplification factor of the signal processing. We do not consider here the effects of thresholds and nonlinearity in amplification factor,[10−12] which however can be incorporated into the model by assuming additional functional dependence of A on C_G.

In the absence of odorants, $P_1(t) = 1 - P_0(t)$. It is easy to use this condition in eq 2 and solve for $P_0(t)$ at arbitrary time. However, the focus of the present work is the average steady state limit behavior, which can be found by imposing the condition that the rates of population changes are zero. Let us denote the concentration of the G-protein in this limit as C_G^s. Then, from the condition that $dP_0(t)/dt = 0$, it is easy to show that the corresponding population of OR_G in the steady state limit becomes

$$P_1^s = \frac{C_G^s}{K_G + C_G^s} \tag{4}$$

where K_G is the equilibrium constant for the OR_G to dissociate into OR and G-protein, and is defined as

$$K_G = \frac{k_G^b}{k_G^f} \tag{5}$$

Given that the steady state limit of eq 2 is established faster than any other processes and is maintained during the majority of signaling time, which is reasonable to assume considering the disparity between the time scale of OR activation (typically in microseconds) and perception time (typically in milliseconds), we find that

$$S_b^s = \frac{A C_G^s k_G^f K_G}{K_G + C_G^s} \tag{6}$$

It is reasonable to assume that the basal signal occurs far from the saturation limit of the G-protein concentration and thus $C_G^s/K_G \ll 1$ because, otherwise, a significant portion of ORs would be unavailable for detecting odorants. Therefore, this condition seems to be required for an OR to function well. The illustration of an effective free energy profile along the line I in Figure 1b is consistent with this situation.

Kinetics with Odorants. In the presence of odorants, we assume that association of OR with G-protein virtually shuts off its chance to bind the odorant. This assumption is reasonable considering recent evidence that association of G-protein with GPCR results in substantial structural change of the latter.[45] Thus, the schematic shown in Figure 2b serves as the only mechanism for the formation of OR_{OG}. This assumption also simplifies the overall kinetics significantly. However, we want to clarify that, pending further evidence, relaxing this assumption may be necessary for certain kinds of ORs, such as broadly responsive ORs.[9]

We also assume that k_D (see Figure 2b) is sufficiently large so that the diffusion process of odorants is not a rate limiting step. In other words, we focus our attention here to only those odorants mobile and small enough to be characterized mainly by the nature of their interactions with the OR. Thus, we consider only the following set of four rate equations:

$$\frac{dP_0(t)}{dt} = -k_O^f(\xi) C_O(t) P_0(t) + k_O^b(\xi) P_2(t) - k_G^f C_G(t) P_0(t) + k_G^b P_1(t) \tag{7}$$

$$\frac{dP_1(t)}{dt} = k_G^f C_G(t) P_0(t) - k_G^b P_1(t) \tag{8}$$

$$\frac{dP_2(t)}{dt} = k_O^f(\xi) C_O(t) P_0(t) + k_{OG}^b(\xi) P_3(t) - k_O^b(\xi) P_2(t) - k_{OG}^f(\xi) C_G(t) P_2(t) \tag{9}$$

$$\frac{dP_3(t)}{dt} = k_{OG}^f(\xi) C_G(t) P_2(t) - k_{OG}^b(\xi) P_3(t) \tag{10}$$

In the above equations, the parameter ξ represents all the chemical features of the odorant determining its interaction with a given OR. Thus, the specificity and sensitivity of the odorant for the OR can be quantified once all four rate

DOI: 10.1021/acs.jpcb.7b00486
J. Phys. Chem. B 2017, 121, 1304−1311

constants, $k^{f}_{O}(\xi)$, $k^{b}_{O}(\xi)$, $k^{f}_{OG}(\xi)$, and $k^{b}_{OG}(\xi)$, as functions of ξ, are known.

As depicted by an effective free energy profile along the line II in Figure 1b, it is expected that $k^{f}_{OG}(\xi)$ and $k^{b}_{OG}(\xi)$ are larger than $k^{f}_{O}(\xi)$ and $k^{b}_{O}(\xi)$ for agonists. In principle, all of these rates for a pair of odorant and OR can be determined if a free energy surface profile of the type shown in Figure 1 becomes available through molecular level simulations. This is still a daunting task considering the large number of ORs (~400 for human) and millions of odorants available from the extremely large space of chemical data. The results being presented below provide possible ways to reduce the parameter space and also to utilize experimental information to gain quantitative understanding of the activation kinetics of ORs.

Under the assumption of steady state condition and based on the normalization condition, eq 1, it is easy to find the following steady state populations from the above rate equations:

$$P^{s}_{0}(\xi) = \frac{1}{D(\xi;\, C^{s}_{G},\, C^{s}_{O})} \tag{11}$$

$$P^{s}_{1}(\xi) = \frac{C^{s}_{G}}{K_{G} D(\xi;\, C^{s}_{G},\, C^{s}_{O})} \tag{12}$$

$$P^{s}_{3}(\xi) = \frac{C^{s}_{O} C^{s}_{G}}{K_{O}(\xi) K_{OG}(\xi) D(\xi;\, C^{s}_{G},\, C^{s}_{O})} \tag{13}$$

where $K_{O}(\xi)$ is the equilibrium constant for OR_{O} to dissociate into OR and odorant (Od), and $K_{OG}(\xi)$ is the equilibrium constant for OR_{OG} to dissociate into OR_{O} and G-protein. These are respectively defined as

$$K_{O}(\xi) = \frac{k^{b}_{O}(\xi)}{k^{f}_{O}(\xi)} \tag{14}$$

$$K_{OG}(\xi) = \frac{k^{b}_{OG}(\xi)}{k^{f}_{OG}(\xi)} \tag{15}$$

In addition, the denominator in eqs 11−13 has the following expression:

$$D(\xi;\, C^{s}_{G},\, C^{s}_{O}) = 1 + \frac{C^{s}_{G}}{K_{G}} + \frac{C^{s}_{O}}{K_{O}(\xi)} + \frac{C^{s}_{O} C^{s}_{G}}{K_{O}(\xi) K_{OG}(\xi)} \tag{16}$$

The signal in the presence of odorants is triggered by steps following the release of G-protein, from either OR_{G} or OR_{OG}. Assuming that the signal amplification factor for both processes are the same, we obtain

$$\begin{aligned} S^{s}_{O}(\xi) &= A(k^{b}_{G} P^{s}_{1}(\xi) + k^{b}_{OG}(\xi) P^{s}_{3}(\xi)) \\ &= \frac{A C^{s}_{G}(k^{f}_{G} K_{O}(\xi) + C^{s}_{O} k^{f}_{OG}(\xi))}{K_{O}(\xi) D(\xi;\, C^{s}_{G},\, C^{s}_{O})} \end{aligned} \tag{17}$$

As the concentration of the odorant increases, the above signal strength approaches the following maximum:

$$S^{s,\max}_{O}(\xi) = \frac{A C^{s}_{G} k^{f}_{OG}(\xi)}{1 + C^{s}_{G}/K_{OG}(\xi)} \tag{18}$$

By using the relation between C^{s}_{G} and S^{s}_{b}, which can be obtained from eq 6, we find that the above result can be expressed as

$$S^{s,\max}_{O}(\xi) = \frac{\alpha(\xi) S^{s}_{b}}{1 + \beta(\xi) S^{s}_{b}} \tag{19}$$

where $\alpha(\xi) = k^{f}_{OG}(\xi)/k^{f}_{G}$ and $\beta(\xi) = (1/K_{OG}(\xi) - 1/K_{G})/(A k^{f}_{G})$. This expression is indeed consistent with a recent experimental result[9] that shows correlation between $S^{s,\max}_{O}(\xi)$ and S^{s}_{b}. Figure 3 shows the fit of the experimental data using

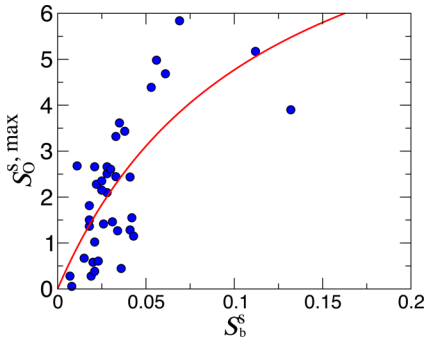

Figure 3. Experimental ratio of maximal odor signal to basal signal, which were taken from Figure 4b of ref 9 and the fit based on eq 19 with $\alpha(\xi) = 89.3$ and $\beta(\xi) = 8.74$.

$\alpha(\xi) = 89.3$ and $\beta(\xi) = 8.74$. One can interpret the fitted value of $\alpha(\xi)$ as indicating that OR_{G} has about a factor of 100 higher rate than the bare OR to bind the G-protein, which is reasonable. The scatter of the experimental data are for many different types of odorants, and thus reflect the fact that $\alpha(\xi)$ and $\beta(\xi)$ in fact vary with each odorant. Nonetheless, overall, eq 19 nicely captures the hyperbolic increase of the total odor response with the basal activity.

Odor Activity. Since the strength of signal generated from OSN is proportional to the net concentration of adenylyl cyclase type III (ACIII) induced through stimulatory G-proteins,[49] it is likely that the activity of an odorant is determined by the difference between $S^{s}_{O}(\xi)$ and S^{s}_{b}, not the ratio. Thus, subtracting eq 6 from eq 17 and dividing the difference with the amplification factor A, we can define the following odor activity (OA):

$$\begin{aligned} a_{O}(\xi) &\equiv \frac{S^{s}_{O}(\xi) - S^{s}_{b}}{A} \\ &= \frac{C^{s}_{G} C^{s}_{O}}{K_{O}(\xi) D(\xi;\, C^{s}_{G},\, C^{s}_{O}) D(\xi;\, C^{s}_{G},\, 0)} \\ &\quad \times \left[k^{f}_{OG}(\xi) - k^{f}_{G} + \left(\frac{k^{f}_{OG}(\xi)}{K_{G}} - \frac{k^{f}_{G}}{K_{OG}(\xi)} \right) C^{s}_{G} \right] \end{aligned} \tag{20}$$

where the fact that $1 + C^{s}_{G}/K_{G} = D(\xi; C^{s}_{G}, 0)$ has been used. This is the primary outcome of the present model, which we believe will have major role in quantifying the odor sensing for a given pair of odorant and OR. Potential isotope effects on this OA can be explained in terms of their effects on constituting rate constants, $k^{f}_{O}(\xi)$, $k^{b}_{O}(\xi)$, $k^{f}_{OG}(\xi)$, and $k^{b}_{OG}(\xi)$, which can be significant if hydrogen bonds are involved in the activation process.

It is easy to confirm that eq 20 exhibits behavior desired for OA. For a very small odorant concentration C^{s}_{O}, it increases linearly. On the other hand, for a large enough concentration of odorant such that $C^{s}_{O}/K_{O}(\xi) \gg 1$, saturation occurs and the OA becomes insensitive to further increase of the concen-

DOI: 10.1021/acs.jpcb.7b00486
J. Phys. Chem. B 2017, 121, 1304−1311

tration. These are all consistent with the features of experimental signals[9,27,50] obtained for ORs with the variation of odorants. This also explains mechanisms of how a given odorant can work as either agonist or antagonist. More detailed account of key qualitative features reflected in the OA is provided in the next section.

QUANTITATIVE CRITERIA

A simple inspection of eq 20 suggests that the case with small $K_O(\xi)$ and large $k^f_{OG}(\xi)$ can produce agonistic behavior. On the other hand, the case of small $k^f_{OG}(\xi)$ is expected to result in antagonistic or inverse agonistic behavior. Indeed, a careful examination of eq 20 shows that these criteria can be made more quantitative. Using the condition for the OA to be positive, we can find the following general criterion for the odorant to be an agonist.

$$\frac{k^f_{OG}(\xi)}{k^f_G} > \frac{K_G(K_{OG}(\xi) + C^s_G)}{K_{OG}(\xi)(K_G + C^s_G)} \tag{21}$$

Considering the hypothetical G-protein saturation limit of $C^s_G \gg K_G$, K_{OG}, the above criterion for agonist becomes the following inequality that depends only on the type of odorant.

$$\frac{k^f_{OG}(\xi)}{k^f_G}\frac{K_{OG}(\xi)}{K_G} = \frac{k^b_{OG}}{k^b_G} > 1 \tag{22}$$

In order to check the validity of the criterion, eq 22, we have plotted eq 20 assuming $C^s_G\, k^f_{OG}(\xi) = 10^3\ s^{-1}$ and $C^s_G k^f_G = 10\ s^{-1}$, for which the criterion for agonist is $K_G/K_{OG} < 100$. The results are shown in Figure 4a. Indeed, for the cases where $K_G/K_{OG} = 1$ and 10, agonistic behavior can be seen for sufficiently large value of C^s_G. On the other hand, for the borderline situation of $K_G/K_{OG} = 100$, we find that the agonistic behavior can be observed only for an optimum value of C^s_G on the order of K_G. Finally, for $K_G/K_{OG} = 1000$ clear inverse agonistic behavior can be seen. Figure 4b shows sections along the coordinate of C^s_O/K_O, for $C^s_G/K_G = 0.01$, which is far from the saturation limit noted above. If we assume that $C^s_G \approx 10\,000$/cell based on the information on yeast cell,[51] which corresponds to $C^s_G \approx 10\,000/(100\ \mu m^3) \approx 10\ \mu M$, this choice amounts to $K_G \approx 5\ \mu M$, which is reasonable.

The behavior observed in Figure 4a can be understood as follows. For the case where $k^b_{OG} > k^b_G$, binding of odorant enhances the signal processing rate for the G-protein bound OR. Thus, providing sufficient number of G-proteins in the vicinity of OR can guarantee increase of signals. On the other hand, for $k^b_{OG} < k^b_G$, an opposite effect will occur. The most interesting case is $k^b_{OG} \sim k^b_G$, where the agonistic behavior is possible only for certain optimum range of C^s_G. These results suggest that three types of odorants are expected based on their dependences on C^s_G as follows: (i) agonistic for sufficient concentration of G-proteins; (ii) partially agonistic only for optimal concentration of G-proteins; (iii) antagonistic or inverse agonistic. Figure 4c shows the effects of C^s_G for a fixed value of $C^s_O/K_O = 0.03$, which clearly demonstrates the three types of dependence on C^s_G.

MICHAELIS–MENTEN FORM

For the purpose of interpreting experimental data with varying odorant concentration, it is convenient to convert eq 20 to the following Michaelis–Menten form:

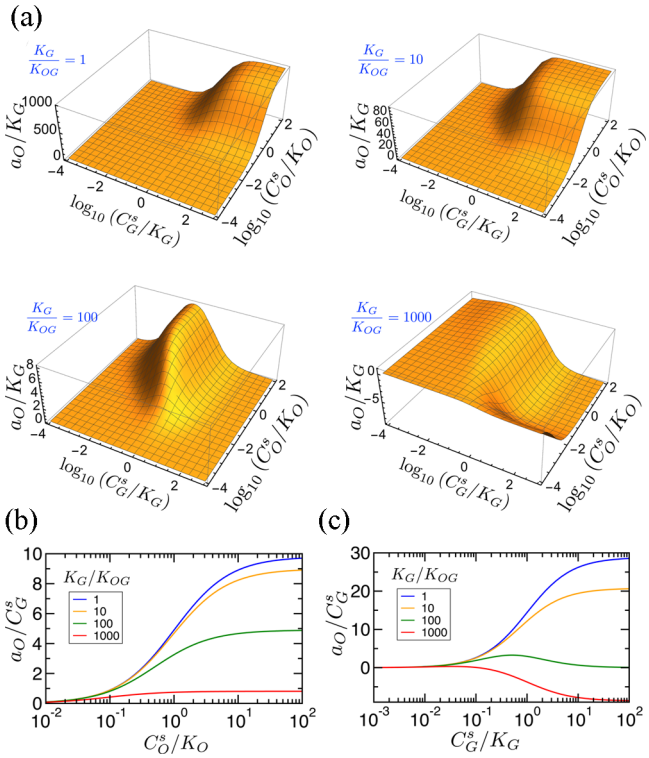

Figure 4. (a) Two dimensional plots of $a_O(\xi)$ with respect to C^s_G/K_G and C^s_O/K_O for four represented values of K_G/K_{OG} for $C^s_G\, k^f_{OG}(\xi) = 10^3\ s^{-1}$, and $C^s_G\, k^f_G = 10\ s^{-1}$. (b) Sections along the coordinate of C^s_O/K_O for the four different values of K_G/K_{OG} at $C^s_G/K_G = 0.01$. (c) Sections along the coordinate of C^s_G/K_G for the four different values of K_G/K_{OG} at $C^s_O/K_O = 0.03$.

$$\frac{a_O(\xi)}{a^m_O(\xi)} = \frac{C^s_O}{EC_{50}(\xi) + C^s_O} \tag{23}$$

where the $EC_{50}(\xi)$ represents the potency of the odorant and $a^m_O(\xi)$, the maximum odor activity, reflects the efficacy of the OR activation. These are respectively given by

$$EC_{50}(\xi) = \frac{K_O(\xi)K_{OG}(\xi)}{K_G}\frac{(K_G + C^s_G)}{(K_{OG}(\xi) + C^s_G)} \tag{24}$$

$$a^m_O(\xi) = \frac{C^s_G K_{OG}(\xi)}{D(\xi, C^s_G, 0)(K_{OG}(\xi) + C^s_G)} \times \left[k^f_{OG}(\xi) - k^f_G + \left(\frac{k^f_{OG}(\xi)}{K_G} - \frac{k^f_G}{K_{OG}(\xi)}\right)C^s_G\right] \tag{25}$$

We have also calculated $EC_{50}(\xi)$ values with the variation of C^s_G, given by eq 24. The results are plotted in Figure 5.

As we have mentioned above (in the last paragraph in Kinetics without Odorants Section), the fraction of OR being combined with the G-protein in the absence of odorants, under normal biological condition, is expected to be small and thus $C^s_G/K_G \ll 1$. Let us assume that this condition and the inequality of eq 22 hold true. In addition, let us assume that $k^f_{OG}(\xi) \gg k^f_G$. Under these three conditions, it is easy to show that

$$\frac{k^f_{OG}(\xi)}{k^f_G} \gg \frac{C^s_G}{K_{OG}(\xi)} \tag{26}$$

DOI: 10.1021/acs.jpcb.7b00486
J. Phys. Chem. B 2017, 121, 1304–1311

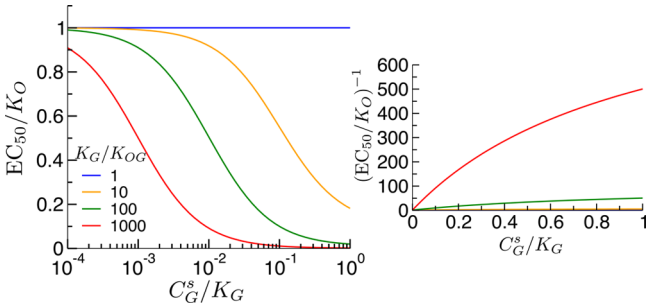

Figure 5. EC_{50} normalized by K_O as a function of G-protein concentration (C^s_G/K_G) for varying K_G/K_{OG} = 1 − 1000. The inset on the right side represents the same data but plots $1/EC_{50}$ instead.

and that eq 20 can be approximated as

$$a_O(\xi) \approx \frac{C^s_G C^s_O k^f_{OG}(\xi) K_{OG}(\xi)}{K_O(\xi)K_{OG}(\xi) + C^s_O(K_{OG}(\xi) + C^s_G)} \tag{27}$$

For the above case,

$$\frac{1}{EC_{50}(\xi)} \approx \frac{1}{K_O(\xi)} + \frac{C^s_G}{K_O(\xi)K_{OG}(\xi)} \tag{28}$$

$$\frac{1}{a^m_O(\xi)} \approx \frac{1}{k^f_{OG}(\xi)K_{OG}(\xi)} + \frac{1}{k^f_{OG}(\xi)C^s_G} \tag{29}$$

The inset in Figure 5 confirms the linear behavior of eq 28 for small C^s_G. These results suggest that extrapolations of the experimental data of $1/EC_{50}(\xi)$ vs C^s_G and those of $1/a^m_O(\xi)$ vs $1/C^s_G$ can be used to obtain the information on $K_O(\xi)$, $K_{OG}(\xi)$, and $k^f_{OG}(\xi)$.

CONCLUSION

In this work, we have presented a simple kinetic model for olfactory activation, nature's versatile and effective tool for chemical recognition. We have defined an odor activity as a normalized difference between the signal generated from the active forms of ORs in the presence of odorants and the basal signal coming from ORs in the absence of odorants. The odor activity represented by eq 20 is our primary result, and establishes a clear quantitative relationship between kinetic/thermodynamic constants for the binding of odorants, G-protein, and OR with the detection signal. Most of all, the expression can serve as a unified framework to represent all the agonistic, partially agonistic, and antagonistic (or inverse agonistic) behavior of odorants.

For agonists, eq 20 exhibits sigmoidal behavior (in the logarithmic scale of odorant concentration), as seen typically in experimental data,[9,27,50] for a sufficient level of G-protein concentration. For antagonists or inverse agonists, the signal remains virtually flat or becomes negative with the increase of odorant concentration, depending on the concentration of G-proteins. This also shows that the distinction between antagonistic and inverse agonistic behavior is of quantitative nature rather than being qualitative. For the borderline case between the agonistic and antagonistic (or inverse agonistic) cases, we have identified an interesting pattern of partial agonism, namely, being active only within a narrow range of G-protein concentrations. Experimental evidence for this behavior is available for D_2 dopamine receptor with various G-proteins.[52] Our model suggests that similar behavior may be found for ORs. Thus, confirmation of this will serve as an important test of our kinetic model. Another important test of our model is the analysis of the experimental EC_{50} value and the maximum signal based on eqs 24 and 25. These expressions can be simplified further to eqs 28 and 29 in the regime of low G-protein concentrations, which are expected around ORs. These expressions can be used to extract the information on relevant kinetic and thermodynamic constants directly from the extrapolation of experimental data.

Another implication of the present work is that seemingly complex and huge chemical space of odorants can be reduced substantially by representing them with much smaller parameter space of rate and equilibrium constants. In other words, the types of odorants with respect to a particular OR can be classified according to their values of rate constants. This will also provide more quantitative means to determine agonistic behavior of odorants. Although the present model was focused on *in vivo* odor activity, the model can be adapted easily to represent *in vitro* experiments as well. This is important considering the availability of a large set of *in vitro* measurement data.[27,53,54]

Finally, we would like to clarify that further refinement and modification of the present kinetic model is expected as more experimental and computational data become available. Some of the potentially important factors that need to be understood better include the nonlinearity in signal production following G-protein activation,[10−12] complication of kinetics due to the involvement of arrestins,[55] and the possibility of multiple kinetic pathways, for example, preactivation of ORs before binding with odorants and dissociation of odorant from OR while being bound to G-protein. Incorporation of these features into a new but more complex kinetic model is feasible and will be the subject of future theoretical investigation.

AUTHOR INFORMATION

Corresponding Author

*E-mail: Seogjoo.Jang@qc.cuny.edu.

ORCID

Seogjoo Jang: 0000-0002-9975-5504

Changbong Hyeon: 0000-0002-4844-7237

Notes

The authors declare no competing financial interest.

ACKNOWLEDGMENTS

The support for S.J. came from the National Science Foundation (CHE-1362926). Authors acknowledge computational support by the Center for Computational Infrastructure for the Sciences at Queens College and the Center for Advanced Computation in Korea Institute for Advanced Study. S.J. thanks Eva Rivera, Daniel Montemayor, Kevin Ryan, Hiro Matsunami, and Eric Block, and C.H. thanks Wonseok Hwang and Jihyun Bak for helpful discussion and comments.

REFERENCES

(1) Zarzo, M. The sense of smell: Molecular basis of odorant recognition. *Biol. Rev.* **2007**, *82*, 455−479.

(2) DeMaria, S.; Ngai, J. The cell biology of smell. *J. Cell Biol.* **2010**, *191*, 443−452.

(3) Mori, K.; Sakano, H. How is the olfactory map formed and interpreted in the mammalian brain? *Annu. Rev. Neurosci.* **2011**, *34*, 467−499.

(4) Park, J. H.; Morizumi, T.; Li, Y.; Hong, J. E.; Pai, E. F.; Hofmann, K. P.; Choe, H.-W.; Ernst, O. P. Opsin, a structural model for olfactory receptors? *Angew. Chem., Int. Ed.* **2013**, *52*, 11021−11024.

DOI: 10.1021/acs.jpcb.7b00486
J. Phys. Chem. B 2017, 121, 1304−1311

(5) Don, C. G.; Riniker, S. Scents and sense: In silico perspectives on olfactory receptors. *J. Comput. Chem.* **2014**, *35*, 2279−2287.
(6) Gelis, L.; Wolf, S.; Hatt, H.; Neuhaus, E. M.; Gerwert, K. Prediction of a ligand binding niche within a human olfactory receptor by combining site-directed mutagenesis with dynamic homology modeling. *Angew. Chem., Int. Ed.* **2012**, *51*, 1274−1278.
(7) Sekharan, S.; Ertem, M. Z.; Zhuang, H.; Block, E.; Matsunami, H.; Zhang, R.; Wei, J. N.; Pan, Y.; Batista, V. S. QM/MM model of the mouse olfactory receptor MOR244−3 validated by site-directed mutagenesis experiments. *Biophys. J.* **2014**, *107*, L5−8.
(8) de March, C. A.; Yu, Y.; Ni, M. J.; Adipietro, K. A.; Matsunami, H.; Ma, M.; Golebiowski, J. Conserved residues control activation of mammalian G-protein coupled odorant receptors. *J. Am. Chem. Soc.* **2015**, *137*, 8611−8616.
(9) Yu, Y.; de March, C. A.; Ni, M. J.; Adipietro, K. A.; Golebiowski, J.; Matsunami, H.; Ma, M. Responsiveness of G protein-coupled odorant receptors is partially attributed to the activation mechanism. *Proc. Natl. Acad. Sci. U. S. A.* **2015**, *112*, 14966−14971.
(10) Bhandawat, V.; Reisert, J.; Yau, K.-Y. Elementary response of olfactory receptor neurons to odorants. *Science* **2005**, *308*, 1931−1934.
(11) Bhandawat, V.; Reisert, J.; Yau, K.-Y. Signaling by olfactory receptor neurons near threshold. *Proc. Natl. Acad. Sci. U. S. A.* **2010**, *107*, 18682−18687.
(12) Ben-Chaim, Y.; Cheng, M. M.; Yau, K.-W. Unitary response of mouse olfactory receptor neurons. *Proc. Natl. Acad. Sci. U. S. A.* **2011**, *108*, 822−827.
(13) Bushdid, C.; Magnasco, M. O.; Vosshall, L. B.; Keller, A. Humans can discriminate more than 1 trillion olfactory stimuli. *Science* **2014**, *343*, 1370−1372.
(14) Meister, M. On the dimensionality of odor space. *eLife* **2015**, *4*, e07865.
(15) Gerkin, R.; Castro, J. B. The number of olfactory stimuli that humans can discriminate is still unknown. *eLife* **2015**, *4*, e08127.
(16) Moncrieff, R. W. A new theory of odour. *Perfumary and Essential Oil Record* **1949**, *40*, 279−285.
(17) Amoore, J. E. Stereochemical theory of olfaction. *Nature* **1963**, *198*, 271−272.
(18) Beets, M. G. J. Structure and odor. In *Molecular structure and organoleptic quality*; Society of Chemical Industry: London, 1957.
(19) Dyson, G. M. The scientific basis of odor. *J. Soc. Chem. Ind., London* **1938**, *57*, 647−651.
(20) Wright, R. H. Odour and chemical constitution. *Nature* **1954**, *173*, 831.
(21) Wright, R. H. Odour and molecular vibration. *Nature* **1961**, *190*, 1101−1102.
(22) Wright, R. H. Neural coding of olfactory information. *J. Theor. Biol.* **1977**, *64*, 473−510.
(23) Sell, C. S. *Chemistry and the sense of smell*; Wiley: Hoboken, NJ, 2014.
(24) Henzler-Wildman, K.; Kern, D. Dynamical personalities of proteins. *Nature* **2007**, *450*, 964−972.
(25) Shukla, D.; Hernández, C. X.; Weber, J. K.; Pande, V. S. Markov state models provide insights into dynamic modulation of protein function. *Acc. Chem. Res.* **2015**, *48*, 414−422.
(26) Plattner, N.; Noé, F. Protein conformational plasticity and complex ligand-binding kinetics explored by atomistic simulations and Markov models. *Nat. Commun.* **2015**, *6*, 7653.
(27) Block, E.; Jang, S.; Matsunami, H.; Sekharan, S.; Dethier, B.; Ertem, M. Z.; Gundala, S.; Pan, Y.; Li, S.; Li, Z.; et al. Implausibility of the vibrational theory of olfaction. *Proc. Natl. Acad. Sci. U. S. A.* **2015**, *112*, E2766−E2774.
(28) Turin, L. A spectroscopic mechanism for primary olfactory reception. *Chem. Senses* **1996**, *21*, 773−791.
(29) Franco, M. I.; Turin, L.; Mershin, A.; Skoulakis, E. M. C. Molecular vibration-sensing component in Drosophila melanogaster olfaction. *Proc. Natl. Acad. Sci. U. S. A.* **2011**, *108*, 3797−3802.
(30) Gane, S.; Georganakis, D.; Maniati, K.; Vamvakias, M.; Ragoussis, N.; Skoulakis, E. M. C.; Turin, L. Molecular vibration-sensing component in human olfaction. *PLoS One* **2013**, *8*, e55780.
(31) Brookes, J. C.; Hartoutsiou, F.; Horsfield, A. P.; Stoneham, A. M. Could humans recognize odor by phonon assisted tunneling? *Phys. Rev. Lett.* **2007**, *98*, 038101.
(32) Solov'yov, I. A.; Chang, P.-Y.; Schulten, K. Vibrationally assisted electron transfer mechanism of olfaction: myth or reality? *Phys. Chem. Chem. Phys.* **2012**, *14*, 13861−13871.
(33) Bittner, E. R.; Madalan, A.; Czader, A.; Roman, G. Quantum origins of molecular recognition and olfaction in drosophila. *J. Chem. Phys.* **2012**, *137*, 22A551.
(34) Moser, C. C.; Keske, J. M.; Warncke, K.; Farid, R. S.; Dutton, P. L. Nature of biological electron transfer. *Nature* **1992**, *355*, 796−802.
(35) Gray, H. B.; Winkler, J. R. Electron transfer in proteins. *Annu. Rev. Biochem.* **1996**, *65*, 537−561.
(36) Jortner, J.; Bixon, M. *Adv. Chem. Phys., Vol. 106, Parts 1 and 2: Electron Transfer From Isolated Molecules to Biomolecules*; John Wiley & Sons, Inc.: NewYork, 1999.
(37) Block, E.; Jang, S.; Batista, V.; Zhuang, H.; Matsunami, H. Vibrational theory of olfaction is implausible. *Proc. Natl. Acad. Sci. U. S. A.* **2015**, *112*, E3155.
(38) Vosshall, L. B. Laying a controversial smell theory to rest. *Proc. Natl. Acad. Sci. U. S. A.* **2015**, *112*, 6525−6526.
(39) Keller, A.; Vosshall, L. B. A psychophysical test of the vibrational theory of olfaction. *Nat. Neurosci.* **2004**, *7*, 337−338.
(40) Glowacki, D. R.; Harvey, J. N.; Mulholland, A. J. Taking Ockham's razor to enzyme dynamics and catalysis. *Nat. Chem.* **2012**, *4*, 169−176.
(41) Layfield, J. P.; Hammes-Schiffer, S. Hydrogen tunneling in enzymes and biomimetic models. *Chem. Rev.* **2014**, *114*, 3466−3494.
(42) de March, C. A.; Kim, S.-K.; Antonczak, S.; Goddard, W. A.; Golebiowski, J. G protein-coupled odorant receptors: From sequence to structure. *Protein Sci.* **2015**, *24*, 1543−1548.
(43) Huang, W.; Manglik, A.; Venkatakrishnan, A. J.; Laeremans, T.; Feinberg, E. N.; Sanborn, A. L.; Kato, H. E.; Livingston, K. E.; Thorsen, T. S.; Kling, R. C.; et al. Structural insights into μ-opioid receptor activation. *Nature* **2015**, *524*, 315−321.
(44) Sounier, R.; Mas, C.; Steyaert, J.; Laeremans, T.; Manglik, A.; Huang, W.; Kobilka, B. K.; Déméné, H.; Granier, S. Propagation of conformational changes during μ-opioid receptor activation. *Nature* **2015**, *524*, 375−378.
(45) Manglik, A.; Kim, T. H.; Masureel, M.; Altenbach, C.; Yang, Z.; Hilger, D.; Lerch, M. T.; Kobilka, T. S.; Thian, F. S.; Hubbell, W. L.; et al. Structural insights into the dynamic process of β_2-Adrenergic receptor signaling. *Cell* **2015**, *161*, 1101−1111.
(46) Dror, R. O.; Pan, A. C.; Arlow, D. H.; Borhani, D. W.; Maragakis, P.; Shan, Y.; Xu, H.; Shaw, D. E. Pathway and mechanism of drug binding to G-protein-coupled receptors. *Proc. Natl. Acad. Sci. U. S. A.* **2011**, *108*, 13118−13123.
(47) Lee, Y.; Kim, S.; Choi, S.; Hyeon, C. Ultraslow water-mediated transmembrane interactions regulate the activation of A_{2A} Adenosine Receptor. *Biophys. J.* **2016**, *111*, 1180−1191.
(48) Lee, Y.; Choi, S.; Hyeon, C. Communication over the network of binary switches regulates the activation of A_{2A} Adenosine Receptor. *PLoS Comput. Biol.* **2015**, *11*, e1004044.
(49) Berbari, N. F.; O'Connor, A. K.; Haycraft, C. J.; Yoder, B. K. The primary cilium as a complex signaling center. *Curr. Biol.* **2009**, *19*, R526−R535.
(50) Belloir, C.; Miller-Leseigneur, M.-L.; Neiers, F.; Briand, L.; Le Bon, A-M. Biophysical and functional characterization of the human olfactory receptor OR1A1 expressed in a mammalian inducible cell line. *Protein Expression Purif.* **2017**, *129*, 31−43.
(51) BNID 107680. Milo, R.; Jorgensen, P.; Moran, U.; Weber, G.; Springer, M. Bionumbers - the database of key numbers in molecular and cell biology. *Nucleic Acids Res.* **2010**, *38*, D750−D753.
(52) Senogles, S. E.; Spiegel, A. M.; Padrell, E.; Iyengar, R.; Caron, M. G. Specificity of receptor-G protein interactions. *J. Biol. Chem.* **1990**, *265*, 4507−4514.
(53) Peterlin, Z.; Li, Y.; Sun, G.; Shah, R.; Firestein, S.; Ryan, K. The importance of odorant conformation to the binding and activation of a representative olfactory receptor. *Chem. Biol.* **2008**, *15*, 1317−1327.

DOI: 10.1021/acs.jpcb.7b00486
J. Phys. Chem. B 2017, 121, 1304−1311

(54) Saito, H.; Chi, Q.; Zhuang, H.; Matsunami, H.; Mainland, J. D. Odor coding by a mammalian receptor repertoire. *Sci. Signaling* **2009**, *2*, ra9.
(55) Mashukova, A.; Spehr, M.; Hatt, H.; Neuhaus, E. M. β-arrestin2-mediated internalization of mammalian odor receptors. *J. Neurosci.* **2006**, *26*, 9902−9912.

DOI: 10.1021/acs.jpcb.7b00486
J. Phys. Chem. B 2017, 121, 1304−1311